

# Current-driven instability of magnetic jets

A. Bonanno<sup>1,2</sup>, V. Urpin<sup>1,3</sup>

<sup>1</sup>) INAF, Osservatorio Astrofisico di Catania, Via S.Sofia 78, 95123 Catania, Italy

<sup>2</sup>) INFN, Sezione di Catania, Via S.Sofia 72, 95123 Catania, Italy

<sup>3</sup>) A.F.Ioffe Institute of Physics and Technology and Isaac Newton Institute of Chile, Branch in St. Petersburg, 194021 St. Petersburg, Russia

May 31, 2019

## ABSTRACT

*Context.* MHD instabilities can be responsible for the complex morphology of astrophysical jets.

*Aims.* We consider the stability properties of jets containing both the azimuthal and axial field of subthermal strength. The presence of the magnetic field with complex topology in jets is suggested by theoretical models and it is consistent with recent observations.

*Methods.* Stability is discussed by means of a linear analysis of the ideal MHD equations.

*Results.* We argue that, in the presence of azimuthal and axial magnetic fields, the jet is always unstable to non-axisymmetric perturbations. Stabilization does not occur even if the strengths of these field components are comparable. If the axial field is weaker than the azimuthal one, instability occurs for perturbations with any azimuthal wave number  $m$ , and the growth rate reach a saturation value for small values of  $m$ . If the axial field is stronger than the toroidal one, the instability shows off for perturbations with relatively large  $m$ .

**Key words.** MHD - instabilities - stars: pre-main sequence - ISM: jets and outflows - galaxies: jets

## 1. Introduction

The magnetic field plays a key role in the formation and propagation of astrophysical jets. Polarization measurements provide important information on orientation and degree of the order of the magnetic field which seems to be highly organized on large scale in many jets (see, e.g., Cawthorne et al. 1993, Leppänen, Zensus & Diamond 1995, Gabuzda 1999, Gabuzda et al. 2004, Kharb et al. 2008). To explain the observational data, simplified models of the three-dimensional magnetic field distribution have been proposed (see, for example, Laing 1981, 1993, Pushkarev et al. 2005, Laing et al. 2006). In particular the polarization data suggest that the magnetic field has a significant transverse component in the main fraction of the jet volume. In accordance with the "traditional" interpretation (see, e.g., Laing 1993), this magnetic structure can be associated with a series of shocks along the jet which enhances the local transverse field. However, VLBI observations of BL Lac 1803+784 (Hirabayashi et al. 1998) revealed that the transverse magnetic structure can be formed by a large scale toroidal magnetic field, and indeed recent observations of a radio jet in the galaxy CGCG 049-033 also reveal the presence of a predominantly toroidal magnetic field (Bagchi et al. 2007, Laing et al. 2006).

Magnetic structures with a significant toroidal field component are predicted by several theoretical models for jet formation (Blandford & Payne 1982, Romanova & Lovelace 1992,

Koide, Shibata & Kudoh 1998). In particular some models of the jet propagation (see, e.g., Begelman, Blandford & Rees 1984) propose that the toroidal field decays more slowly than the poloidal one as a function of the distance from the central object, therefore the toroidal field should eventually become dominant. Other generation mechanisms based either on the combined influence of turbulence and large-scale shear (see, e.g. Urpin 2006) or on dynamo action along with magneto-centrifugal and reconnection processes (de Gouveia Dal Pino, 2005) also predict the occurrence of a significant toroidal component. A situation where loops of toroidal magnetic field dominate the field distribution would produce important dynamical consequences for the jet structure, for instance, providing pressure confinement through magnetic tension forces (Chan & Henriksen 1980, Eichler 1993). However it is well known from plasma physics (see, e.g., Kadomtzev 1966) that the toroidal magnetic field may cause various MHD instabilities even in simple cylindrical configurations.

In general, different types of instabilities can be present in astrophysical jets. They can be caused by boundary effects, shear, stratification, magnetic fields, and are also likely to be responsible for the observed morphological complexity of jets. For this reason several analytical (see, e.g., Ferrari, Trussoni & Zaninetti 1980, Bodo et al. 1989, 1996, Hanasz, Sol & Sauty 1999; see also Birkinshaw 1997 for a review) and numerical (Hardee et al. 1992, Appl 1996, Lucek & Bell 1996, Min 1997, Kudoh, Matsumoto & Shibata 1999) works have been devoted

to the study of the stability properties of jets. A systematic study of the Kelvin-Helmholtz instability in nonrelativistic jets with the longitudinal magnetic field has been performed by Bodo et al. (1989, 1996) where the effect of rotation was also included. In particular several unstable modes including a slow mode associated with the presence of the magnetic field and an inertial mode caused by rotation have been found. Shear-driven instabilities also can be very important in jets (Urpin, 2002). Numerical simulations (Aloy et al. 1999a, 1999b) indicate that the radial structure of jets may be more complex with a transition shear layer surrounding the jet core. The thickness of the shear layer depends on the distance being around 20% of the jet radius near the nozzle but broadening near the head where it is of the order of the jet radius. This shear layer may have an important consequence for various properties of jets including their stability (see, e.g., Hanasz & Sol 1996, 1998, Aloy & Mimica 2008).

In this paper, we consider the instability associated with the topology of the magnetic field in jets. Magnetic fields generated by the dynamo action or by hydrodynamic motions can be topologically non-trivial and thus prone to pressure-driven or current-driven instabilities (see, e.g., Longaretti 2008 for review). This problem is well studied in the context of experiments on controlled thermonuclear fusion (see, e.g., Bateman 1978) and it has been discussed in relation to jets by a number of authors (see, e.g., Eichler 1993, Appl 1996, Appl et al. 2000, Lery et al. 2000, Baty & Keppens 2002). A linear stability analysis of supermagnetosonic jets has been performed by Appl et al. (2000) for different magnetic configurations including a force-free field. It has been shown that the current-driven instabilities can occur in the presence of the axial field for various profiles of the azimuthal field even if these components are comparable. The non-linear development of the current-driven instability has been analysed by Lery et al. (2000) who found that this instability can modify the magnetic structure of a jet redistributing the current density in the inner part. The current-driven instability of relativistic jets and plerions in the presence of toroidal magnetic field has been considered by Begelman (1998) who obtained that the dominant instability in this case are the kink ( $m = 1$ ) and pinch ( $m = 0$ ) modes. The kink mode generally dominates, thus destroying the concentric field structure. Note that numerical simulations often support the idea that magnetic jets should be unstable and can generate turbulent motions due to instabilities. For instance, Lery & Frank (2000) have found that the instabilities seen in their jet simulations develop with a wavelength and growth time that are well matched by a linear stability analysis. Relativistic simulations of extragalactic jets by Leismann et al. (2005) and Roca-Sogorb et al. (2008) also clearly show that the various irregularities develop in the jet flow can be interpreted as MHD instabilities.

Our study focuses on the stability of jets with a subthermal magnetic field where the magnetic energy is lower than the thermal energy of particles. Such magnetic field can be generated, for instance, by the turbulent dynamo action or by hydrodynamic motion (stretching) in the process of jet propagation. We show that stability properties of jets with a subthermal field can be essentially different from those with a highly superthermal force-free magnetic field considered by Appl et al. (2000).

In particular, higher azimuthal modes with  $m \gg 1$  can have the strongest growth rate at variance with the superthermal case.

The paper is organized as follows. Section 1 is devoted to the introduction, section 2 contains the derivation of the relevant equations, and section 3 shows the numerical results. Conclusions are presented in section 4.

## 2. Basic equations

We consider a very simplified model assuming that the jet is an infinitely long stationary cylindrical outflow and its propagation through the ambient medium is modeled by a sequence of quasi-equilibrium states. For the sake of simplicity, it is assumed often that the velocity within a jet does not depend on coordinates (see, e.g., Appl 1996, Appl et al. 2000, Lery et al. 2000), and we will adopt the same assumption in our study. Then, we can treat stability in the rest frame of the jet. We explore the cylindrical coordinates  $(s, \varphi, z)$  with the unit vectors  $(\mathbf{e}_s, \mathbf{e}_\varphi, \mathbf{e}_z)$ . The magnetic field is assumed to be axisymmetric with non-vanishing  $z$ - and  $\varphi$ -component. The azimuthal field depends on the cylindrical radius alone,  $B_\varphi = B_\varphi(s)$ , but the axial magnetic field  $B_z$  is constant in our model.

Since the magnetic field is subthermal, we can use the MHD equations in the incompressible limit

$$\frac{\partial \mathbf{v}}{\partial t} + (\mathbf{v} \cdot \nabla) \mathbf{v} = -\frac{\nabla P}{\rho} + \frac{1}{4\pi\rho} (\nabla \times \mathbf{B}) \times \mathbf{B}, \quad (1)$$

$$\nabla \cdot \mathbf{v} = 0, \quad (2)$$

$$\frac{\partial \mathbf{B}}{\partial t} - \nabla \times (\mathbf{v} \times \mathbf{B}) = 0, \quad (3)$$

$$\nabla \cdot \mathbf{B} = 0. \quad (4)$$

In the basic state, the gas is assumed to be in hydrostatic equilibrium in the radial direction, then

$$\frac{\nabla P}{\rho} = \frac{1}{4\pi\rho} (\nabla \times \mathbf{B}) \times \mathbf{B} \quad (5)$$

Stability will be studied by making use of a linear perturbative analysis. Since the basic state is stationary and axisymmetric, the dependence of perturbations on  $t$ ,  $\varphi$ , and  $z$  can be taken in the form  $\exp(\sigma t - ik_z z - im\varphi)$  where  $k_z$  is the wavevector in the axial direction and  $m$  is the azimuthal wavenumber. Small perturbations will be indicated by subscript 1, while unperturbed quantities will have no subscript. Then, the linearized Eqs. (1)-(4) read

$$\sigma \mathbf{v}_1 = -\frac{\nabla P_1}{\rho} + \frac{1}{4\pi\rho} [(\nabla \times \mathbf{B}_1) \times \mathbf{B} + (\nabla \times \mathbf{B}) \times \mathbf{B}_1], \quad (6)$$

$$\nabla \cdot \mathbf{v}_1 = 0, \quad (7)$$

$$\sigma \mathbf{B}_1 - (\mathbf{B} \cdot \nabla) \mathbf{v}_1 + (\mathbf{v}_1 \cdot \nabla) \mathbf{B} = 0, \quad (8)$$

$$\nabla \cdot \mathbf{B}_1 = 0. \quad (9)$$

Eliminating all variables in favor of the radial velocity perturbation  $v_{1s}$ , we obtain

$$\begin{aligned} & \frac{d}{ds} \left[ \frac{1}{\lambda} (\sigma^2 + \omega_A^2) \left( \frac{dv_{1s}}{ds} + \frac{v_{1s}}{s} \right) \right] - k_z^2 (\sigma^2 + \omega_A^2) v_{1s} \\ & - 2\omega_B \left[ k_z^2 \omega_B (1 - \alpha) - \frac{m(1 + \lambda)}{s^2 \lambda^2} \left( 1 - \frac{\alpha \lambda}{1 + \lambda} \right) (\omega_{Az} + 2m\omega_B) \right. \\ & \quad \left. - \frac{m\omega_{Az}}{s^2 \lambda^2} \right] v_{1s} + \frac{4k_z^2 \omega_A^2 \omega_B^2}{\lambda(\sigma^2 + \omega_A^2)} v_{1s} = 0, \quad (10) \end{aligned}$$

where

$$\begin{aligned} \omega_A &= \frac{1}{\sqrt{4\pi\rho}} \left( k_z B_z + \frac{m}{s} B_\varphi \right), \quad \omega_{Az} = \frac{k_z B_z}{\sqrt{4\pi\rho}}, \\ \omega_B &= \frac{B_\varphi}{s \sqrt{4\pi\rho}}, \quad \alpha = \frac{\partial \ln B_\varphi}{\partial \ln s}, \quad \lambda = 1 + \frac{m^2}{s^2 k_z^2}. \end{aligned}$$

This equation was first derived by Bonanno & Urpin (2008b) in their analysis of the non-axisymmetric stability of stellar magnetic configurations. For axisymmetric perturbations ( $m = 0$ ), Eq. (10) recovers Eq. (11) of the paper by Bonanno & Urpin (2008a). It represent a non-linear eigenvalue problem for  $\sigma$  which can be solved once the boundary conditions are given. We assume that  $v_{1s}$  should be finite at the jet axis. As far as the outer boundary is concerned, it is rather difficult to formulate a plausible boundary condition because, in fact, there is no boundary between the jet and ambient medium. Nevertheless, we mimic the presence of this boundary by supposing  $v_{1s} = 0$  at the jet radius  $s = s_1$ . Note that we also tried other outer boundary conditions (for example, with  $v_{1s} \neq 0$ ), but the results did not change qualitatively.

We can represent the azimuthal magnetic field as

$$B_\varphi = B_{\varphi 0} \psi(s), \quad (11)$$

where  $B_{\varphi 0}$  is the characteristic field strength and  $\psi \sim 1$ . To calculate the growth rate of the instability, it is convenient to introduce dimensionless quantities

$$x = \frac{s}{s_1}, \quad q = k_z s_1, \quad \Gamma = \frac{\sigma}{\omega_{B0}}, \quad \omega_{B0} = \frac{B_{\varphi 0}}{s_1 \sqrt{4\pi\rho}}, \quad \varepsilon = \frac{B_z}{B_{\varphi 0}}. \quad (12)$$

Then, Eq. (10) reads

$$\begin{aligned} & \frac{d}{dx} \left( \frac{dv_{1s}}{dx} + \frac{v_{1s}}{x} \right) + \left( \frac{dv_{1s}}{dx} + \frac{v_{1s}}{x} \right) \frac{d \ln \Delta}{dx} - q^2 \left( 1 + \frac{m^2}{q^2 x^2} \right) v_{1s} - \\ & \frac{2q^2 \psi(x)}{x(\Gamma^2 + f^2)} \left\{ \left[ \left( 1 - \frac{m^2}{q^2 x^2} \right) \frac{\psi(x)}{x} - \frac{m\varepsilon}{qx^2} \right] (1 - \alpha) - \frac{2mf}{m^2 + q^2 x^2} \right\} v_{1s} \\ & + \frac{4q^2 f^2 \psi^2(x)}{x^2(\Gamma^2 + f^2)^2} v_{1s} = 0, \quad (13) \end{aligned}$$

where

$$f = q\varepsilon + m \frac{\psi(x)}{x}, \quad \Delta = \frac{q^2 x^2 (\Gamma^2 + f^2)}{m^2 + q^2 x^2}. \quad (14)$$

We thus solve Eq. (13) for a wide range of the parameters and different functional dependence  $\psi(x)$ .

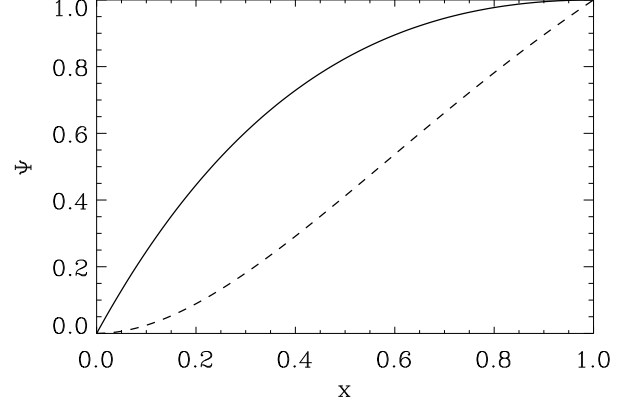


**Fig. 1.** The dependence of  $\psi$  on  $x$  for  $p = 1$  and  $n = 1$  (solid line) and 2 (dashed line).

### 3. Numerical results

We assume that the function  $\psi(s)$ , determining the dependence of the azimuthal magnetic field on the radial coordinate, is given by

$$\psi(s) = x^n e^{-p(x-1)}, \quad (15)$$

where  $n$  and  $p$  are the parameters. In addition,  $\psi$  goes to 0 at the jet axis and is equal to 1 at the surface  $x = 1$ . For the purpose of illustration, we plot  $\psi(x)$  for  $p = 1$  and  $n = 1, 2$  in Fig. 1. These two distributions of  $B_\varphi$  are qualitatively different because the case  $n = 1$  corresponds to the magnetic configuration with non-vanishing current density at the jet axis whereas this quantity goes to 0 in the case  $n = 2$ . The total axial current, integrated over the jet section, is same for both cases. The distributions with  $n = 1$  and  $n = 2$  represent jet models with current densities relatively smoothed or concentrated to the outer boundary, respectively.

Eq. (13) together with the given boundary conditions is two-point boundary value problem which can be solved by using the “shooting” method (Press et al. 1992). In order to solve Eq. (13), we used a fifth-order Runge-Kutta integrator embedded in a globally convergent Newton-Rawson iterator. We have checked that the eigenvalue was always the fundamental mode because the corresponding eigenfunction had no zero except that at the boundaries.

In Fig. 2, we plot the dependence of the growth rate on the axial wavevector for the magnetic configuration with non-vanishing current at the axis and a relatively weak axial magnetic field,  $\varepsilon = B_z/B_{\varphi 0} = 0.1$ . As it was noted by Bonanno & Urpin (2008), the presence of an axial field breaks symmetry between positive and negative values of the axial wavevector  $q$  in Eq. (13) even if  $B_z$  is small compared to  $B_\varphi$ . However, Eq. (13) still contains some degeneracy because it is invariant under  $(m, q) \rightarrow (-m, -q)$  or  $(m, \varepsilon) \rightarrow (-m, -\varepsilon)$  transformation. The instability occurs only for perturbations with  $q$  within a narrow range that depends on the azimuthal wavenumber  $m$ . For example, perturbations with  $m = 1$  and  $m = 6$  are unstable if  $0 > q > -70$  and  $-60 > q > -200$ , respectively. Note that

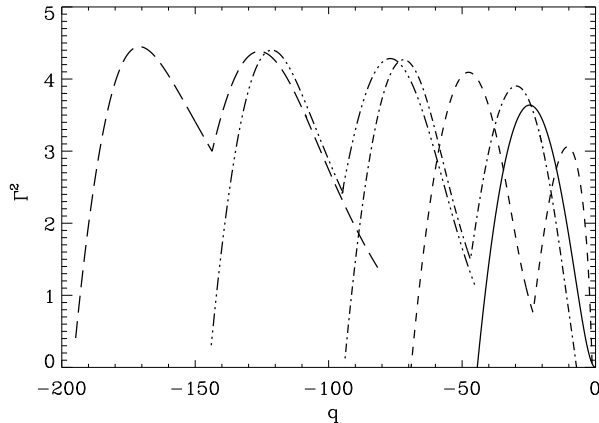


**Fig. 2.** The dependence of the normalized growth rate of instability on the wavevector  $q$  for  $\varepsilon = 0.1$ ,  $p = 1$  and  $n = 1$ . Different types of lines correspond to different azimuthal wavenumbers:  $m = 0$  (solid),  $m = 1$  (dashed),  $m = 2$  (dot-and-dashed),  $m = 4$  (dot-dot-dashed), and  $m = 6$  (long-dashed).

the unstable perturbations with positive  $m$  should have negative  $q$  and, on the contrary, if  $m$  is negative, instability occurs only for perturbations with positive  $q$ .

The growth rate has two clear maxima with the highest maximum corresponding to  $q \sim -m/\varepsilon$ . By the order of magnitude, the axial wave-vector of the most rapidly growing perturbation can be estimated from the condition of magnetic resonance

$$\omega_A = \frac{1}{\sqrt{4\pi\rho}} \left( k_z B_z + \frac{m}{s} B_\phi \right) \approx 0. \quad (16)$$

Indeed, this equation implies  $\omega_A \propto q\varepsilon + m\psi(x) \approx 0$ . Since  $\psi(x) \sim 1$  in our model, the condition  $\omega_A = 0$  corresponds to

$$q \sim -m/\varepsilon. \quad (17)$$

The most rapidly growing modes turn out to be highly anisotropic if the axial field is weak compared to the toroidal one: their axial wavelength  $\lambda_z = 2\pi/k_z \sim 2\pi\varepsilon s$  is much shorter than the radial and azimuthal lengthscale. The growth rate is rather high and it is of the order of the inverse Alfvén time scale. The growth rate slowly increases with  $m$  and perturbations with a shorter azimuthal scale grow faster. The axisymmetric mode ( $m = 0$ ) turns out to be the most slowly growing.

The model with  $n = 2$  exhibits the similar behaviour of perturbations. As mentioned, electric currents are more concentrated near the outer boundary in this model. The values of  $q$  that allow the instability are smaller in this case and, hence, the corresponding vertical wavelengths are longer but the range of unstable  $q$  is narrower. For the considered values of  $m$ , the growth rate is approximately smaller by a factor 2. The general impression is that the configuration with currents concentrated closer to the outer boundary is a more stable than the one with a more uniformly distributed currents.

In Fig.4 we plot the growth rate of instability for the configuration with the axial field much weaker than the toroidal one,  $\varepsilon = 0.01$ . The distribution of the toroidal field is given by

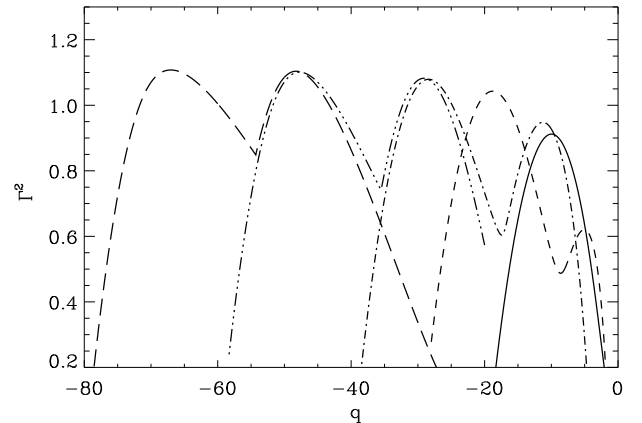


**Fig. 3.** Dependence of the normalized growth rate of instability on the wavevector  $q$  for  $\varepsilon = 0.1$ ,  $p = 1$  and  $n = 2$ . Different types of lines correspond to the same azimuthal wavenumbers as in Fig.2.

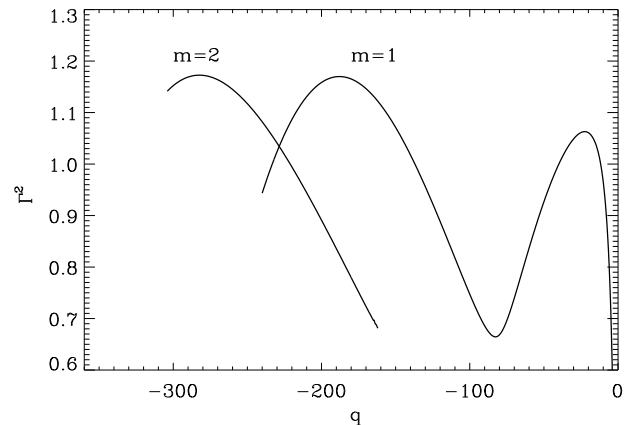


**Fig. 4.** Growth rate as a function of  $q$  for  $\varepsilon = 0.01$  and distribution of the toroidal field (15) with  $p = 1$  and  $n = 2$ .

Eq. (15) with  $p = 1$  and  $n = 2$ . The instability can occur in this case as well, but only perturbations with very large  $q$  can be unstable. Even for the mode  $m = 1$ , the growth rate reaches its maximum at  $q \approx 200$ . For modes with larger  $m$ , the maximum growth rate corresponds to substantially larger values of  $q$  (very short axial wavelengths). Unfortunately, our numerical code does not allow to resolve the modes with a very short axial wavelength, and we were able to extend our calculations only to  $q \approx 300$ . It is worth noticing that even perturbations with such large  $q$  still grow rapidly and the growth rate is of the order of the inverse Alfvén time.

Fig.5 shows the growth rate versus  $q$  for a larger ratio of the axial and toroidal fields ( $\varepsilon = 0.5$ ) and for the model with  $p = 1$  and  $n = 2$ . In this case, the instability occurs at substantially smaller values of  $q$  and, correspondingly, at longer axial wavelength. The modes with small  $m$  grow relatively slowly, but the growth rate increases with increasing  $m$ . The mode with  $m = 8$  has the growth rate comparable to the inverse Alfvén time, but the modes with larger  $m$  are growing even faster. In that sense,

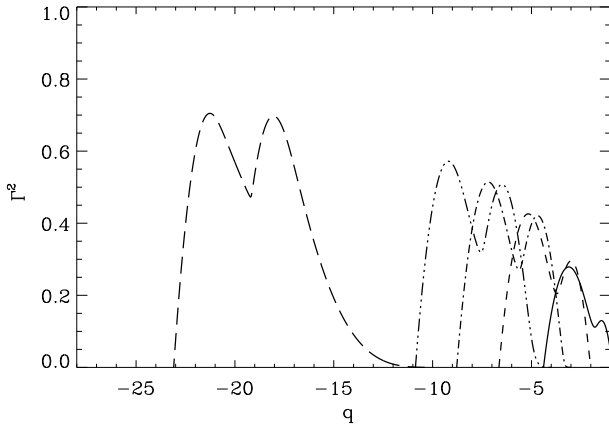


**Fig. 5.** Growth rate as a function of  $q$  for  $\varepsilon = 0.5$ ,  $p = 1$  and  $n = 2$ . The curves correspond to  $m = 1$  (solid),  $m = 2$  (short-dashed),  $m = 3$  (dot-and-dashed),  $m = 4$  (dot-dot-dashed) and  $m = 8$  (long-dashed).

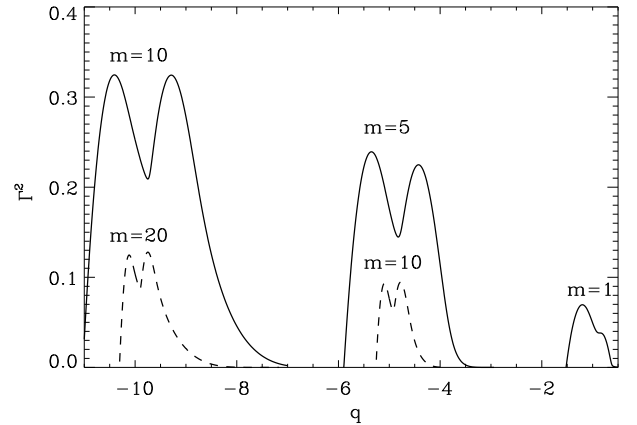


**Fig. 6.** A comparison of the growth rate for the cases  $\varepsilon = 1$  (solid) and 2 (dashed). The parameters determining the distribution of the toroidal field are  $p = 1$  and  $n = 2$ .

the dependence of modes on  $m$  in the cases  $\varepsilon \sim 1$  and  $\varepsilon < 1$  seems to be qualitatively similar.

Fig. 6 compares the growth rates for the cases  $\varepsilon = 1$  and 2. We have considered the model with  $p = 1$  and  $n = 2$ , but the behaviour is qualitatively the same for other models. The growth rates are generally smaller than in the previous cases ( $\varepsilon < 1$ ), but the instability is still present. A suppression of the growth rate is certainly more pronounced if  $\varepsilon = 2$ . However, even in this case,  $\Gamma$  increases relatively rapidly with increasing  $m$  and it is likely to reach a saturation value  $\sim 1$  at sufficiently large  $m$ . The values of  $q$  that correspond to unstable perturbations are smaller than in Fig. 2-5. Fig. 6 illustrates very well the fact that the instability cannot be completely suppressed even if the axial field is sufficiently strong and  $\varepsilon > 1$ . At large  $\varepsilon$ , the instability is not very efficient ( $\Gamma^2 > 0$  but very small) for perturbations with not very large  $m$  but those with large  $m$  can still reach a saturation value of  $\Gamma^2 \sim 0.1$ . Indeed in the specific case of  $\varepsilon = 2$  we could not find significant growth rate for modes with  $m \leq 5$ , but we found that the growth rate is of the order of the inverse Alfvén crossing time for sufficiently high azimuthal wavenumbers.

To illustrate how velocity perturbations depend on the cylindrical radius, in Fig. 7 the eigenfunctions for one of the models shown in Fig. 6 ( $\varepsilon = 1$ ) are plotted. The eigenfunctions correspond to the azimuthal wavenumbers  $m = 1$  (solid), 5 (dashed), and 10 (dot-and-dashed). The  $m = 1$  mode is the only mode that does not go to zero at the jet axis. Typically, the modes reach their maximum closer to the outer boundary, and an increase of  $m$  results in the eigenfunctions that are more and more localized. For large  $m$ , motions in the core region of the jet are substantially suppressed. This sharpness of the eigenfunctions is the main reason of the problems in numerical calculations for high  $m$ .

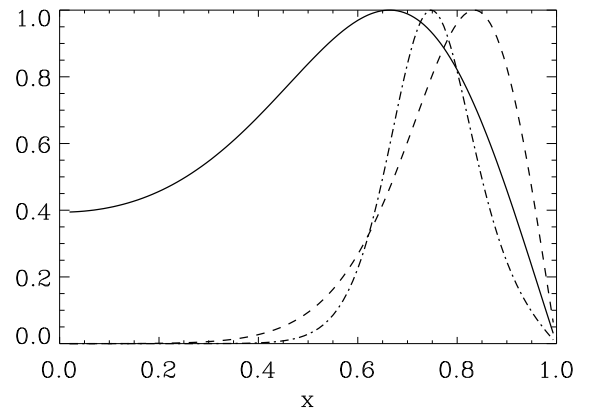


**Fig. 7.** The eigenfunctions for the model with  $\varepsilon = 1$ ,  $p = 1$ , and  $n = 2$ . The curves correspond to  $m = 1$  (solid),  $m = 5$  (dashed), and  $m = 10$  (dot-and-dashed).

#### 4. Discussion

We have considered the instability that can occur in jets if the magnetic field has a relatively complex structure with non-vanishing azimuthal and axial components. The presence of the magnetic field with complex topology is suggested by both the theoretical models for jet formation and the mechanisms of generation of the magnetic field. Our study considers only jets with subthermal magnetic fields as the stability properties of jets with superthermal fields can be essentially different (Appl et al. 2000).

It turns out that the magnetic jet is always unstable if the azimuthal field increases to the outer boundary. This fact does not depend on the ratio of the axial and azimuthal fields. However, the character of the instability can be essentially different for different  $\varepsilon$ . If the axial field is weaker than the azimuthal one and  $\varepsilon < 1$ , then the growth rate tends to a saturation value of the order of the inverse of few Alfvén crossing times for  $m > 1$ . Our code does not allow us to calculate eigenfunc-

tions and eigenvalues for very large  $m$  in this case but Fig. 2 and 3 indicates that the growth rate shows a saturation trend for  $m \gg 1$ . In this case the fastest growing mode has the axial wavevector  $k_z \sim -m/\varepsilon s$  that is determined by the condition of magnetic resonance. This wavevector which corresponds to the axial wavelength  $\lambda_z = 2\pi/|k_z| \sim (2\pi\varepsilon)(s/m)$ . At small  $\varepsilon$ , the axial wavelength of the most rapidly growing perturbations should be very small. Therefore, if the longitudinal magnetic field is weaker than the azimuthal one, we expect that the instability generates structures in jets with very short length scale in  $z$ -direction. Note that such a behaviour can cause problems in numerical modelling of the instability because a very high resolution in the axial direction is required.

When the ratio of the axial and azimuthal fields becomes comparable to or greater than 1, the behaviour of the instability as a function of  $m$  is qualitatively similar although the growth rate is significantly smaller. In this case perturbations with relatively small  $m$  are substantially suppressed but we still find a numerical evidence for a saturation trend as we increase  $m$  although it is reached for much larger values of  $m$  than in the  $\varepsilon < 1$  case. It is important to stress that even  $m \sim 100$  in the azimuthal direction is still a macroscopic scale, and dissipative effects are negligible in this case.

To the best of our knowledge, the conclusion that the instability can arise even if  $\varepsilon \geq 1$  with a characteristic azimuthal wavenumber  $m \gg 1$  is new and at variance with the widely accepted opinion that magnetic configurations should be stabilized at  $B_z \sim B_\varphi$ .

It would be important to investigate the consequences of our findings for jets by performing more realistic numerical simulations, we hope to address this question in the near future.

## Acknowledgement

One of the authors (VU) thanks INAF-Osservatorio Astrofisico di Catania for hospitality and financial support. We would like to thank L.Santagati for careful reading the manuscript.

## References

- Aloy M.A., Ibáñez J.M., Martí J.M., Müller E. 1999a. *ApJS*, 122, 151  
Aloy M.A., Ibáñez J.M., Martí J.M., Müller E. 1999b. *ApJ*, 523, L125  
Aloy M., Mimica P. 2008. *ApJ*, 681, 84  
Appl S. 1996. *A&A*, 314, 995  
Appl S., Lery T., Baty H. 2000. *A&A*, 355, 818  
Bagchi J., Gopal-Krishna, Krause M., Joshi S. 2007. *ApJ*, 670, L85  
Bateman G. 1978. *MHD Instabilities*, Cambridge: MIT Press  
Baty H., Keppens R. 2002. *ApJ*, 580, 800  
Begelman M. 1998. *ApJ*, 493, 291  
Begelman M., Blandford R., Rees M. 1984. *Rev. Mod. Phys.*, 56, 255  
Birkinshaw M. 1997. In "Advanced Topics on Astrophysical and Space Plasmas" (Eds. E. Gouveia Dal Pino, A.Peratt, G. Medina Tanco, A.Chian), Dordrecht: Kluwer  
Blandford R., Payne D. 1982. *MNRAS*, 199, 883  
Bodo G., Rosner R., Ferrari A., Knobloch E. 1989. *ApJ*, 341, 631  
Bodo G., Rosner R., Ferrari A., Knobloch E. 1996. *ApJ*, 470, 797  
Bonanno A., Urpin V. 2008a. *A&A*, 477, 35  
Bonanno A., Urpin V. 2008b. *A&A*, 488, 1  
Cawthorne T., Wardle J., Roberts D., Gabuzda D., Brown L. 1993. *ApJ*, 416, 496  
Chan K.L., Henriksen R.N. 1980. *ApJ*, 241, 534  
de Gouveia Dal Pino, E.M., *AdSpR* 35, 908  
Eichler D. 1993. *ApJ*, 419, 111  
Ferrari A., Trussoni E., Zaninetti L. 1980. *MNRAS*, 193, 469  
Hanasz M., Sol H. 1996. *A&A*, 315, 355  
Hanasz M., Sol H. 1998. *A&A*, 339, 629  
Hanasz M., Sol H., Sauty C. 1999. In "Plasma Turbulence and Energetic Particles in Astrophysics" (Eds. M.Ostrowski, R.Schlickeiser), Krakow: Obserwatorium Astronomiczne, Uniwersytet Jagiellonski  
Hardee P., Cooper M., Norman M., Stone J. 1992. *ApJ*, 399, 478  
Hirabayashi H. et al. 1998. *Science*, 281, 1825  
Gabuzda D. 1999. In "Plasma Turbulence and Energetic Particles in Astrophysics" (Eds. M.Ostrowski, R.Schlickeiser), Krakow: Obserwatorium Astronomiczne, Uniwersytet Jagiellonski  
Gabuzda D., Murray E., Cronin P. 2004. *MNRAS*, 351, L89  
Kadomtsev B. In "Reviews in Plasma Physics" (Ed. M.Leontovich), v.2, New York: Consultants Bureau  
Kharb P., Gabuzda D., Shastri P. 2008. *MNRAS*, 384, 230  
Koide S., Shibata K., Kudoh T. 1998. *ApJ*, 495, L63  
Kudoh T., Matsumoto R., Shibata K. 1999. *AdSpR*, 23, 1101  
Laing R.A. 1981. *ApJ*, 248, 87  
Laing R.A. 1993. In "Astrophysical Jets" (Eds. D.Burgarella, M.Livio, C.O'Dea), Cambridge: Cambridge University Press  
Laing R., Canvin J., Bridle A. 2006. *AN*, 327, 523  
Leismann T., Anton L., Aloy M., Müller E., Martí J.M., Miralles J.A., Ibanez J.M. 2005. *A&A*, 436, 503  
Leppänen K., Zensus A., Diamond P. 1995. *AJ*, 110, 2479  
Lery T., Baty H., Appl S. 2000. *A&A*, 355, 1201  
Lery H., Frank A. 2000. *ApJ*, 533, 877  
Longaretti P.-Y. 2008. In "Numerical MHD and Instabilities Lecture Notes in Physics", v. 754, 131, Berlin Springer  
Lucek S.G., Bell A.R. 1996. *MNRAS*, 281, 245  
Min K.W. 1997. *ApJ*, 482, 733  
Press W.H., Teukolsky S.A., Vetterling W.T., Flannery B.P. 1992. *Numerical Recipes in FORTRAN. The art of scientific computing* (Cambridge: UP)  
Pushkarev A., Gabuzda D., Vetikhovskaya Yu., Yakimov V. 2005. *MNRAS*, 356, 859  
Roca-Sogorb M., Perucho M., Gomez J.L., Martí J.M., Anton L., Aloy M., Agudo I. 2008. *astro-ph/0802.3826*  
Romanova M., Lovelace R. 1992. *A&A*, 262, 26  
Urpin V. 2002. *A&A*, 385, 14  
Urpin V. 2006. *A&A*, 455, 779